EFFECTIVE VALUES OF ELECTRODYNAMIC CHARACTERISTICS OF THE PROCESS OF NONCONSUMABLE ELECTRODE WELDING WITH PULSE MODULATION OF ARC CURRENT

V.F. DEMCHENKO, U. BOI, I.V. KRIVTSUN and **I.V. SHUBA**

E.O. Paton Electric Welding Institute, NASU
11 Kazimir Malevich Str., 03680, Kiev, Ukraine. E-mail: office@paton.kiev.ua

The paper is devoted to analysis of the influence of pulse modulation of welding current on effective values of electrodynamic characteristics of the process of nonconsumable electrode welding. The first part of the paper provides analysis of the possibilities for increasing the effective value of arc current through selection of optimum time and current parameters of pulse modulation. A quite general case of current modulation by pulses of trapezoidal shape is considered (rectangular and triangular pulses are treated as particular cases). In the second part distribution of effective values of electromagnetic and dynamic characteristics of modulated current in the weld pool is studied, proceeding from a non-stationary model of arc discharge and model of electromagnetic processes in the metal being welded. Force impact of modulated current on weld pool metal at current modulation by triangular pulses with pauses at 10 kHz frequency is considered as a characteristic example. Influence of dynamic effects in the pulsed arc on distribution of effective values of electromagnetic characteristics, namely centripetal component of Lorenz force and magnetic pressure, is analyzed. A conclusion is made that with optimum shape of current pulses dynamic effects arising in nonstationary arc are capable of essentially enhancing its force impact on weld pool metal in nonconsumable electrode welding with high-frequency current modulation, compared to welding by constant current coinciding in magnitude with effective value of modulated current. 19 Ref., 13 Figures.

K e y w o r d s : *nonconsumable electrode welding, pulse current modulation, electrodynamic characteristics, effective value, weld pool metal, mathematical models*

Pulse modulation of arc current in nonconsumable electrode (TIG) welding is one of the effective methods to control the characteristics of thermal and dynamic impact of the arc on the metal being welded. Variation of the parameters of welding current modulation, such as frequency, relative pulse duration, pulse amplitude and shape, allows changing the depth and shape of metal penetration, and thermal cycle of welding in a broad range, and, therefore, influencing the structure and properties of weld metal and near-weld zone, lowering residual stresses and deformations of welded item. Determination of optimum values of parameters of welding current pulse modulation requires having valid data on relative influence of each of them on the nature of running of thermal, electromagnetic, gas- and hydrodynamic processes in arc plasma and metal being welded.

A large number of works are devoted to experimental study and mathematical simulation of processes running in arc plasma, on the surface and in the volume of metal being welded in TIG welding with pulse modulation of arc current [1–12]. Modes with low-frequency (modulation frequency $F < 10$ Hz) [1, 2, 6, 7, 9, 10], medium frequency ($F \leq 5$ kHz) [2, 4,

5] and high-frequency ($F > 10$ kHz) [2, 3, 8, 11, 12] modulation of welding current, are considered. In the majority of the above-listed publications, however, (except for works [2, 4]) practically no attention is given to studying the influence of current pulse shape on the nature of running of nonstationary processes of heat-, mass- and charge transfer in the considered system, as well as on the effective values of the above process characteristics. Moreover, only low-frequency modulation of arc current is considered in publications devoted to detailed numerical modeling of the process of TIG welding by modulated current [6, 7, 9, 10]. Therefore, the objective of this work is theoretical study and numerical analysis of the influence of the shape of welding current pulses in a broad range of modulation frequencies on effective values of electromagnetic characteristics, determining the thermal, and, particularly, dynamic (force) impact of the arc with refractory cathode on the metal being welded.

Basic postulates. Let $I(t)$ be the periodically changing in time t arc current, assumed to be unidirectional; $\tau = 1/F$ is the current modulation period; $I_A = \langle I \rangle$, $I_E = \sqrt{\langle I^2 \rangle}$ is its average and effective values, respectively. Here and furtheron $\langle \phi \rangle$ means integral mean value of function $\phi(t)$ in the range of $[0, \tau]$:

$$\langle \phi \rangle = \frac{1}{\tau} \int_0^\phi \phi(t)dt.$$

Effective value of alternating current is usually understood to be such a value of constant current, which creates a thermal effect, coinciding with thermal effect of alternating current. At constant ohmic resistance R of the conducting medium thermal power W, generated by constant current I, is expressed in terms of the square of current, according to Joule–Lenz law: $W = I^2 R$. Then, in keeping with the above interpretation of effective value of alternating current, the following equality holds: $W = W_E$, where $W_E = I_E^2 R$ is the effective thermal power of alternating current.

In the case of nonconsumable electrode welding with pulse current modulation, this interpretation of the effective value of current is valid only at consideration of the processes of current transfer and heat input in the metal being welded, specific electric resistance of which is weakly dependent on the value of flowing current. At the same time, because of the high electric conductivity of metals, thermal effect of current flowing in the metal being welded, turns out to be insignificant. Therefore, effective value of current as the determining characteristic of thermal processes in the item being welded, is not significant. In contrast to that, Joule heating of arc plasma has a decisive influence on its thermal state. In keeping with volt-ampere characteristic of the arc, however, arc voltage U (arc gap resistance R) essentially depends on flowing current [3, 13]. Therefore, thermal power W_E of the arc at pulse modulation of current should be determined by averaging the product of arc current and voltage

$$W_E = \langle IU \rangle = \frac{1}{\tau} \int_0^\tau I(t)U(t)dt$$

[3], i.e. in the form, which is not expressed directly through the square of effective current value.

Welding current impact on arc plasma and metal being welded is not exhausted by generation of thermal energy. Another important characteristic of such an impact is electromagnetic force, arising as a result of interaction of arc current with intrinsic magnetic field. The impact of this force is manifested in two ways. On the one hand, the resultant gas-dynamic head of arc plasma flow deforms the free surface of the weld pool, resulting in shifting of the heat source in-depth of the metal being welded, thus promoting increase of penetration depth. On the other hand, electromagnetic force, acting on molten metal in the weld pool, intensifies convective energy transfer from the most heated central part of pool surface to its bottom part that also promotes increase of penetration depth [14].

Let us now consider the thermal and dynamic impact of modulated current on the metal being welded.

For this purpose, we will perform assessment of the time of relaxation of thermal and gas-dynamic states of the metal melt at its disturbance due to external impact, which we will associate with pulsed change of welding current in the context of the discussed problem. Let $\mathrm{Fo}^{(T)} = a\bar{t}/\bar{l}^{\,2}$ and $\mathrm{Fo}^{(V)} = v\bar{t}/\bar{l}^{\,2}$ be the thermal and hydrodynamic Fourier criteria. Here: a is the thermal diffusivity of the metal being welded; v is the coefficient of kinematic viscosity of the melt; $\bar{l}$ is the characteristic geometrical size of the weld pool, $\bar{t}$ is the characteristic time. As is customary, we will assume that during times $\bar{t}^{(T)}$, $\bar{t}^{(V)}$, as which values of criteria $\mathrm{Fo}^{(T)}$ and $\mathrm{Fo}^{(V)}$ reach a unity, relaxation of disturbance of thermal and hydrodynamic state of the metal due to the impact of disturbing external factor, takes place. Selecting the characteristic size of the weld pool $\bar{l} = 0.5$ cm and assuming that for stainless steel, for instance, $a = 0.07$ cm²/s, $v = 0.07$ cm²/s [6], we obtain: $\bar{t}^{(T)}$, $\bar{t}^{(V)} \approx 3.6$ s . These, very approximate calculations, allow assessing the duration of transient processes of heat- and mass-transfer in the weld pool as a value of the order of several seconds. We can confidently say that at modulation frequencies $F \geq 100$ Hz (modulation period $\tau < 10^{-2}$ s) thermal and hydrodynamic processes in the weld pool are sensitive not to current, time-varying characteristics of electromagnetic field, but to their values, averaged over the period of current modulation.

Work [14] also shows that at spot DC TIG welding, volume density of electromagnetic force in the weld pool, excited by electric current flowing through it, is proportional to $I^2(r, z)$, where $\{r, z\}$ is the cylindrical system of coordinates, axis OZ of which is directed normal to the surface of metal being welded; $I(r,z) = 2\pi \int_0^r j_z(r',z)r'dr'$ is the current, flowing within a circle of radius r, selected in an arbitrary axial section z of the pool; $j_z(r, z)$ is the axial component of current density. According to the above-performed evaluation of characteristic times $\bar{t}^{(T)}$, $\bar{t}^{(V)}$, in welding with modulated current of frequency $F > 100$ Hz, force impact of arc current on weld pool metal is expressed through value $\langle I^2(r, z) \rangle$, i.e. it depends on effective value of the square of current, flowing through a circle of the selected radius. Note that unlike determination of effective current value by its thermal effect, this characteristic is in no way connected with ohmic resistance of the metal. Therefore, the notion of effective value of current in TIG welding by modulated current can be given another, more general meaning, based not on thermal but on force impact of current on the metal being welded.

It is obvious that the greater the square of effective value of welding current I_E^2, the larger its distributed

characteristic $\langle I^2(r, z)\rangle$, and the greater the effective force impact of arc current on the metal being welded, respectively. At assigned average value of modulated current I_A its maximum effective value I_E can be achieved by properly selecting the shape and time parameters of the pulses. This problem is considered in the first section of this paper for the general case of welding current modulation by pulses of a trapezoidal shape, particular cases of which are triangular and rectangular pulses. The second section presents the results of numerical analysis of effective (averaged by modulation period) electrodynamic characteristics distributed in the volume of the metal being welded, in TIG welding with pulse modulation of current. At analysis of these results, attention is focused on force impact of arc current on weld pool metal, as well as its influence on the intensity of hydrodynamic flows, excited in it.

1. Effective value of modulated current. Let us consider modulated current $I(t)$ in the form of uni-directional pulses of trapezoidal shape with pauses between them (Figure 1, *a*). Average value of such current can be presented in the form of $I_A = (1 - \alpha)I_1 + \alpha I_2$, where $\alpha = \dfrac{\tau_3 + \tau_2 - \tau_1}{2\tau}$ $(0 \leq \alpha \leq 1)$; $\tau_1, \tau_3 - \tau_2$ are the durations of leading and trailing fronts; $\tau_2 - \tau_1$ is the duration of pulse «plateau», where current is kept constant, equal to I_2; $\tau - \tau_3$ is the duration of the pause (see Figure 1, *a*). Thus, average value of modulated current is expressed in terms of values of current in the pause I_1 and maximum current in the pulse I_2, as well as through dimensionless time parameter α. Let us introduce two more dimensionless parameters: $\xi = \tau_3 / 2\tau$ $(0 < \xi \leq \dfrac{1}{2})$ and $\gamma = (\tau_2 - \tau_1)/\tau_3$ $(0 \leq \gamma \leq 1)$. The first of them characterizes relative pulse duration (mode stiffness) and is connected with relative pulse duration $s = \tau/\tau_3$ by ratio $\xi = 1/2s$, and the second is the relative duration of pulse «plateau» and characterizes its shape (at $\gamma = 0$ trapezoidal pulse becomes a triangular one, and at $\gamma = 1$ it becomes rectangular). As

a result, dimensionless parameter α can be expressed through ξ and γ as follows: $\alpha = \xi(1 + \gamma)$.

For any periodically changing current $I(t)$ the following representation holds:

$$I(t) = I_A = A\eta(t) \tag{1}$$

where $A = I_2 - I_1$ is the amplitude of current variation; $\eta(t)$ is a certain normed function, containing information about the shape and time characteristics of current pulses. According to the definition of average current, function $\eta(t)$ should meet the following condition

$$\int_0^\tau \eta(t)dt = 0. \tag{2}$$

In particular, for a trapezoidal pulse, given in Figure 1, *a*, function $\eta(t)$ has the following form (see Figure 1, *b*):

$$\eta(t) = \begin{cases} \dfrac{t}{\tau_1} - \alpha, & 0 < t < \tau_1; \\ 1 - \alpha, & \tau_1 < t < \tau_2; \\ -\dfrac{t - \tau_2}{\tau_3 - \tau_2} + 1 - \alpha, & \tau_2 < \tau < \tau_3; \\ -\alpha, & \tau_3 < t < \tau. \end{cases} \tag{3}$$

Using representation (1) and condition (2), the following expression for the square of effective current value can be derived:

$$I_E^2 = I_A^2 + A^2 f(\xi, \gamma), \tag{4}$$

where $f(\xi, \gamma) = \langle \eta^2 \rangle$.

Omitting cumbersome calculations, we will give the final expression for function $f(\xi, \gamma)$:

$$f(\xi, \gamma) = \xi\left[\dfrac{2}{3}(1 + 2\gamma) - \xi(1 + \gamma)^2\right],$$

behaviour of which is shown in Figure 2. From the explicit form of this function it follows that effective value of pulsed current depends on relative duration and shape of pulses and does not depend on their repetition rate. We will also note that $f(\xi, \gamma) \geq 0$, i.e. square of effective value of current is higher than average current square.
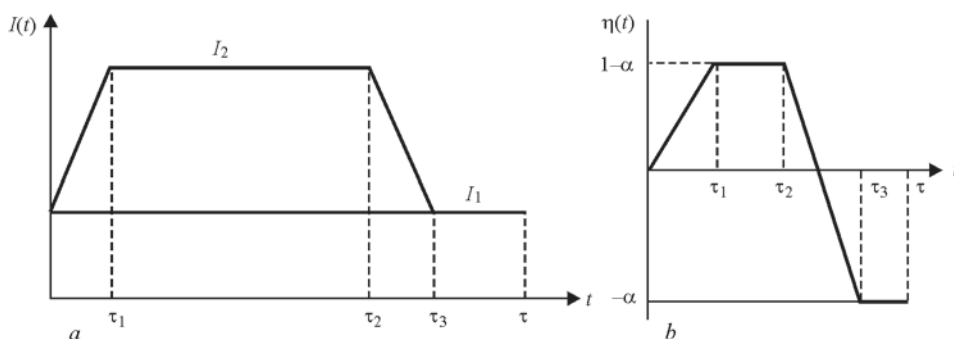

Figure 1. Schematic representation of arc current pulse: *a* — trapezoidal pulse with a pause; *b* — respective normed pulse (function $\eta(t)$)

As follows from expression (4), at specified value of I_A there are two possibilities to increase the effective value of modulated current: the first is through increasing amplitude A; the second — by selection of such values of time parameters of the pulse, at which function $f(\xi, \gamma)$ has the highest value. In the first case, increasing the magnitude of current I_2, in principle, allows reaching as high a value of current I_E as is desired, by reducing pulse duration appropriately, so as to ensure satisfying condition I_A = const. Considering the quadratic dependence of I_E^2 on current amplitude, this method is highly effective. Its application, however, is limited by the capabilities of arc power source (in equipment models known to the authors $I_2 \leq 500$ A [8]). Therefore, it is of interest to consider the second method of increasing I_E.

Furtheron we will assume that values I_1, I_2 (or A), as well as average current value I_A are given and will select parameters ξ, γ so that function $f(\xi, \gamma)$ included into expression (4), had the highest values. Note that at given values I_1, A, I_A, parameter $\alpha = \xi(1+\gamma)$ is uniquely determined: $\alpha = (I_A - I_1)/A$. Therefore, at analysis of numerical values of function $f(\xi, \gamma)$ not the entire range of ξ, γ variation should be considered, but just those of their values, which satisfy equation $\xi(1 + \gamma) = \alpha$. Expressing γ from this equation through ξ, α, and substituting it into the expression for $f(\xi, \gamma)$, we obtain $f(\xi, \alpha) = \frac{4}{3}\alpha - \alpha^2 - \frac{2}{3}\xi$. This function decreases monotonically with ξ increase and has the largest value at minimum value ξ_{min}. In case of triangular pulses ($\gamma = 0$) we find $\xi = \alpha$ from expression $\xi = \alpha/(1 + \gamma)$, and in the case of rectangular pulses ($\gamma = 1$) we have $\xi = \alpha/2$. Thus, minimum value $\xi_{min} = \alpha/2$, providing at given α the largest value of function $f(\xi_{min}, \alpha) = \alpha - \alpha^2$, is reached in the case $\gamma = 1$. Function $\alpha - \alpha^2$ has a maximum at $\alpha = 0.5$, that yields $\xi = 0.25$, i.e. this set of dimensionless parameters corresponds to rectangular pulses in the form of a meander.

Thus, at given I_1, A, I_A, of all the possible variations of the considered forms of the pulse, the largest effective value of current $I_E = \sqrt{I_1^2 + I_1 A + 0.5 A^2}$ is reached at application of rectangular pulses in the form of a meander, average current value being $I_A = I_1 + 0.5A$.

As in practice it is impossible to reach an ideal rectangular shape of pulses, it is of interest to study behaviour of function $f(\xi, \gamma)$ for the general case of trapezoidal current pulse. Let us denote the total duration of the pulse leading and trailing fronts as $\tau_f = \tau_1 + \tau_3 - \tau_2$ (see Figure 1, a), determined by parameters of the power source and electric circuit, containing the welding arc. In the considered case minimum value of ξ is defined as follows: $\xi_{min} = \alpha / (2 - \overline{\tau}_f)$, where $\overline{\tau}_f = \tau_f / \tau_3$, which yields
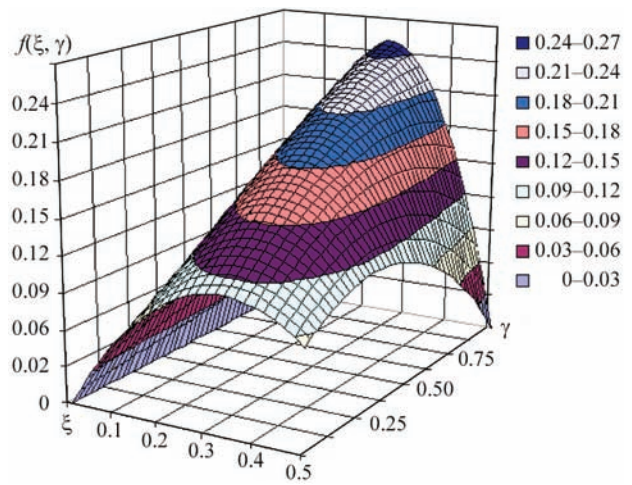

Figure 2. Appearance of function $f(\xi, \gamma)$

$$f(\xi_{min}, \alpha) = \frac{2}{3}\left(2 - \frac{1}{2 - \overline{\tau}_f}\right)\alpha - \alpha^2.$$

This function has a maximum equal to

$$f(\overline{\tau}_f) = \frac{1}{9}\left(2 - \frac{1}{2 - \overline{\tau}_f}\right)^2,$$

at

$$\alpha = \frac{1}{3}\left(2 - \frac{1}{2 - \overline{\tau}_f}\right).$$

As follows from Figure 3, value of function $f(\overline{\tau}_f)$ is rather weakly dependent on total front duration. So, for instance, if τ_f is equal to 50 % of pulse duration, value $f(\overline{\tau}_f)$ decreases just by 20 %, compared to the best value achieved at current modulation by rectangular pulses in the form of a meander ($\overline{\tau}_f$ 0).

2. Distribution of effective values of characteristics of electromagnetic field of arc current in the metal being welded. As was noted above, in TIG welding with current modulation at more than 100 Hz frequency the impact of electromagnetic force on arc plasma and weld pool metal is determined not by current value of electromagnetic force, but by its value, averaged in time over the period of current modulation, i.e., effective value of the force. Expression for vor-
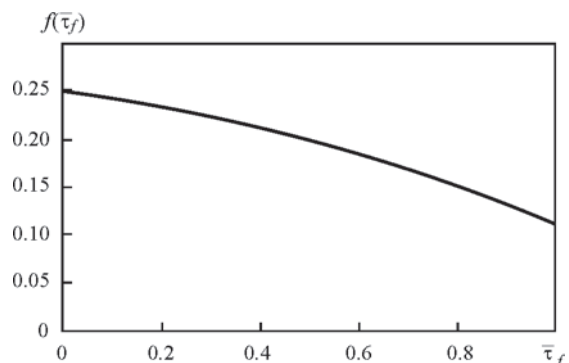

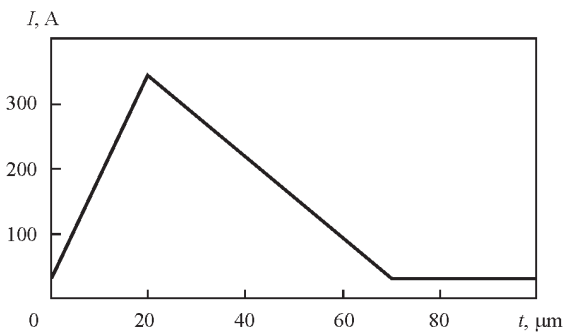**Figure 3.** Influence of relative duration of pulse fronts on $f(\overline{\tau}_f)$

Figure 4. Triangular current pulse with pause

tex component of this force in the cylindrical system of coordinates is written in strict compliance with the one given in [14] for constant current arc with the only difference that $I^2(r, z)$ is replaced by $\langle I^2(r, z)\rangle$, namely

$$\vec{F}_{\text{rot}}(r, z) = -\mu_0\mu \frac{\langle I^2(r, z)\rangle}{4\pi^2 r^3}\vec{e}_r, \qquad (5)$$

here, μ is the metal permeability; μ_0 is the universal magnetic constant; $\vec{e}_r$ is the unit radius-vector.

Proceeding from magnetostatics equations [15], we can show that under the impact of force $\vec{F}_{\text{rot}}(r, z)$ a magnetic pressure field arises in the weld pool, average (over current modulation period) magnitude of which $\langle P_{\text{mag}}(r, z)\rangle$ is determined by the following formula

$$\left\langle P_{\text{mag}}(r, z)\right\rangle = \frac{\mu_0\mu}{4\pi^2}\int_r^\infty \left|\vec{F}_{\text{rot}}(r', z)\right| dr'. \qquad (6)$$

In the approximation of magnetostatics, radial component of magnetic pressure field $\langle P_{\text{mag}}(r, z)\rangle$ is balanced by force $\vec{F}_{rot}(r, z)$, and its axial component is balanced in the full system of equations of hydrodynamics by forces of nonmagnetic origin, primarily, those of inertia and viscosity [14].

We will use expressions (5), (6) for evaluation of effective values of electromagnetic force and magnetic pressure in the metal being welded in spot TIG welding by modulated current. Performance of de-

Figure 5. Change in time of axial current density in the arc anode binding region

tailed calculations requires information about the distribution of current characteristic $I(r, z, t)$ in the metal volume within one period of current modulation. Two mathematical models were developed for this purpose: first is model of the arc, burning in a nonstationary mode; second is the model of electromagnetic processes in the metal being welded in welding by modulated current. Axisymmetric (2D) model of constant current arc [16] was modified [17], allowing for nonstationary nature of thermal and gas-dynamic situation in arc plasma, which is due to a change of electric current in time (in keeping with the assigned shape of the pulse and frequency modulation). Such a model allows modeling the dynamics of burning of a nonstationary arc discharge and obtaining calculated data on time-varying distributed and integral characteristics of the arc column and anode region of the arc, including distribution of electric current density on the surface of metal being welded. Computer realization of the proposed model envisages feeding a packet of pulses in the quantity, sufficient for establishing arc plasma state, recurring from pulse to pulse.

During computational experiments, burning of argon arc 3 mm long with tungsten cathode was studied, anode was assumed to be non-evaporating, pulse current modulation was performed in the form of feeding triangular-shaped pulses with pauses between them (Figure 4) at the following values of current and time parameters of the pulse: $I_1 = 30$ A, $I_2 = 345$ A ($A = 315$ A); $\tau_1 = \tau_2 = 20$ μs, $\tau_3 = 70$ μs, $\tau = 100$ μs ($\xi = 0.35$; $\gamma = 0$), that corresponds to $I_A = 140$ A, $I_E \approx 175$ A; $F = 10$ kHz. Time parameters of this triangular current pulse are practically optimal in the sense that they provide maximum effective value of current at its given average value (see Section 1).

In discussion of the results of calculation of characteristics of modulated current arc, we will give preference to analysis of processes running in arc anode region, disregarding a number of interesting features of nonstationary thermal, gas-dynamic and electromagnetic processes in its column. Let $j_a(r, t)$ be the distribution of axial component of current density at the anode, calculated using arc model [17]. Let us first consider the change in time of axial value of current density $j_a(0, t)$ per one modulation period. In Figure 5 the change of the above characteristic in time (curve *1*) is given in comparison with values of axial density of current for stationary arcs at currents $I = I_2, I_A, I_1$ (curves *2*, *3*, *5*, respectively). The same figure gives axial value of current density averaged over the modulation period (dotted curve *4*). Figure 6 at gives the distributions of current density at the anode in different moments of time for the leading (Figure 6, *a*) and trailing (Figure 6, *b*) fronts of the pulse. Dashed lines
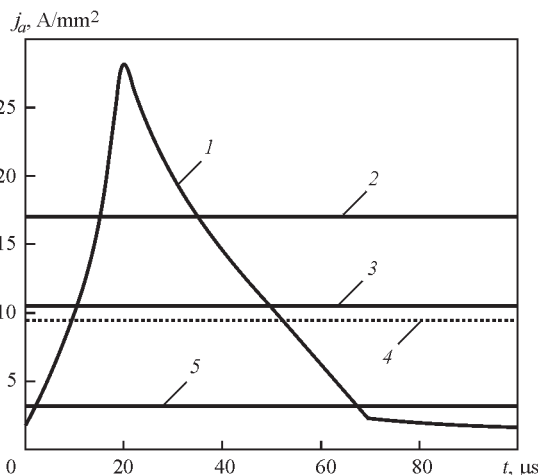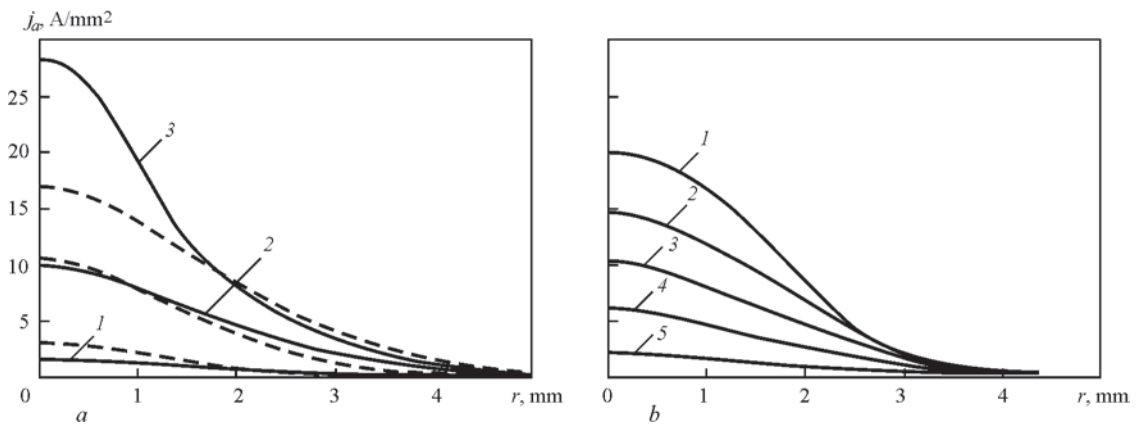
Figure 6. Distribution of current density at the anode at different moments of time: *a* — leading front (*1* — *t* = 0, *I* = 30 A; *2* — *t* = = 10 μs; *I* = 187 A; *3* — *t* = 20 μs, *I* = *345 A); *b* — trailing front (*1* — *t* = 30 μs, *I* = 282 A; *2* — *t* = 40 μs; *I* = 219 A; *3* — *t* = 50 μs, *I* = 156 A; *4* — *t* = 60 μs, *I* = 93 A; *5* — *t* = 70 μs, *I* = 30 A)

in Figure 6, *a* show the respective distributions for constant current arc at *I* = 30, 140 and 345 A.

Before going over to analysis of nonstationary nature of variation of electric current density at the anode, shown in Figures 5, 6 we will give a general description of mode of arcing with high-frequency current modulation. According to the accepted terminology, at current modulation electric processes run in the quasi-stationary mode, if their characteristics change periodically with current modulation frequency, and this change is realized in the mode of successive change of stationary states, corresponding to constant current, which coincides in its magnitude with instantaneous value of modulated current. In the case considered here, the first of these conditions is fulfilled already after feeding the first 5–6 pulses. The second condition, however, is not satisfied at modulation frequencies of 10 kHz. This is clearly demonstrated by the data shown in Figures 5, 6. Effect of pronounced nonstationary nature of variation of electric current density at the anode is manifested in that the maximum value of $j_a(0, t)$ (see Figure 5, curve *1*) is approximately 1.5 times higher than axial density of current at the anode for stationary arc at current *I* = = I_2 = 345 A. The same effect is manifested also in distribution of electric current at the anode (see Figure 6, curve *3* and respective dashed curve). Therefore, we can conclude that in the considered case the arc burns in a nonstationary mode, accompanied by a significant increase of current density at the anode.

The simplest explanation for this effect may be that the rapidly changing current at the pulse leading front (see Figure 4) is passed through the current channel of arc column, the size of which does not have enough time to follow the change of *I*(*t*), because of inertia of gas-dynamic processes in arc plasma, and preserves the dimensions, close to those which it had at the start of modulation period (at small value of current). As shown by analysis of other dynamically changing

characteristics of arc discharge, such a mechanism of increasing electric current density at the anode is not the only one, i.e. there also exist other causes behind the extreme nature of $j_a(0, t)$ variation, and these causes are associated not with arc column, but with near-anode plasma region.

We will consider changes of radial distribution of near-anode plasma temperature $T_a(r, t)$ (Figure 7, *a*) in time within the first 40 μs from the moment of the pulse start, of which 20 μs falls on its leading front. At current *I* = 30 A (*t* = 0) axial value of near-anode plasma temperature is equal to 7736 K (see Figure 7, *a*, curve *1*). At current increase up to 345 A (*t* = 20 μs) the temperature rises up to 8960 K and continues rising over the next 10 μs (temperature distributions at these moments of time are represented in Figure 7, *a* by curves *2*, *3*). Notably, $T_a(r, t)$ increase is limited by a circle, the radius of which does not exceed 3 mm;
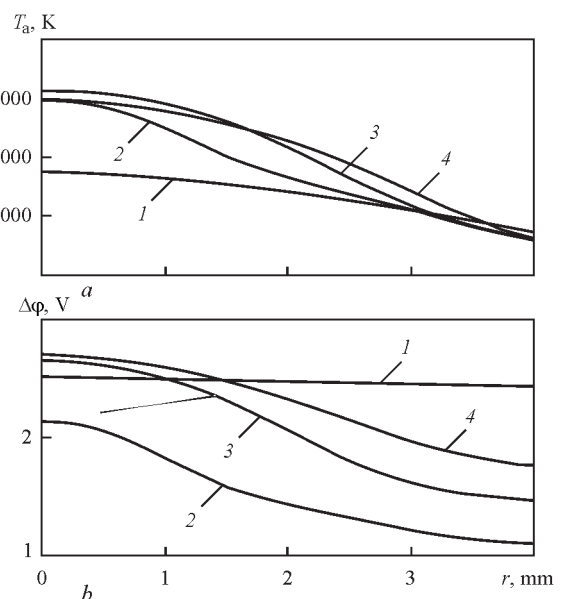

Figure 7. Distribution of temperature (*a*) and potential (*b*) of near-anode plasma along its boundary with arc column: *1* — *t* = = 0, *I* = 30 A; *2* — *t* = 20 μs, *I* = 345 A; *3* — *t* = 30 μs, *I* = 282 A; *4* — *t* = 40 μs, *I* = 219 A

at greater values of r near-anode plasma temperature does not change compared to the temperature it has reached during the pause (as a result of inertia of thermal and gas-dynamic processes in arc column).

Local temperature rise (in time and space) leads to a change of radial distribution of potential drop across the anode $U_a(r, t) = -\Delta\varphi(r, t)$, which depends on distribution of electric current density at the anode and near-anode plasma temperature [16]. This dependence is illustrated by presented in Figure 7, b, results of calculation of the dynamics of distribution of value $\Delta\varphi$, which actually is the near-anode plasma potential on the boundary with arc column, under the condition that anode surface potential is taken to be constant and equal to zero.

At low current $I = 30$ A ($t = 0$) the boundary of near-anode plasma and arc column is practically iso-potential ($\Delta\varphi \approx 2.5$ V — Figure 7, b, curve 1) so that current density vector in it is directed along a normal to anode surface. With increase of axial value of temperature of near-anode plasma by more than 1000 K (see Figure 7, a, curves 2–4), this boundary becomes significantly non-isopotential, and in such a way that potential value decreases along the anode surface, reaching a gradient of about 1 V at 3 mm distance from the center of anode binding region. Non-uniform distribution of anode potential drop in near-anode plasma results in appearance of radial component of current density vector, directed from the center to the periphery of anode region, which enables radial unloading of current flowing out of the anode. The effect of local increase of current density at the anode is achieved exactly due to current flowing more readily out of the anode into arc plasma. The effect of arc current contraction at the anode due to additional local heating of arc plasma was found for the first time in study [8] under the conditions of hybrid (TIG + CO_2-laser) welding.

At the conclusion of this analysis, we will mention one more possible cause for current density increase at high-frequency modulation of current (see Fig-
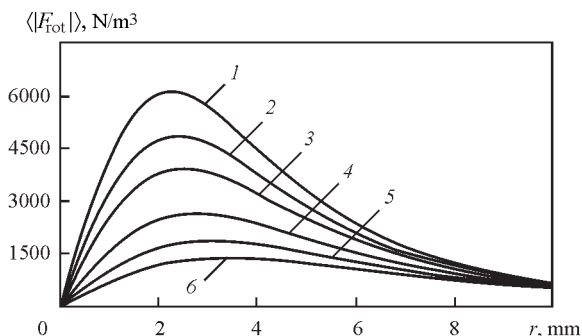

Figure 8. Distribution of effective value of vortex component of electromagnetic force in different axial sections of the plate being welded: 1 — $z = 0$; 2 — 0.25; 3 — 0.5; 4 — 1.0; 5 — 1.5; 6 — 2.0 mm

ures 5, 6). In the region of low temperatures of argon plasma (of the order of 7–12 kK), its specific electric conductivity rises noticeably with temperature increase, while at temperatures above 20 kK plasma electric conductivity is weakly dependent on temperature. Thus, increase of arc plasma temperature at current rise only slightly changes the electrophysical properties of arc column, and at the same time creates a region of increased electric conductivity in paraxial regions of near-anode plasma. Such a feature can also promote increase of current density in the central part of the region of anode binding of the arc.

Now let us go back to the problem of force impact of modulated current on the metal being welded. Calculation of current distribution in 10 mm plate being welded was performed using axisymmetric (2D) model of electric processes described in [14]. For each moment of time t_k during one period of current modulation ($t_k \in [0, \tau]$, $k = 1$–100) distribution of axial current density $j_a(r, t_k)$ was assigned on the anode surface ($z = 0$), which was determined on the basis of a computer model of nonstationary arc for a current pulse, shown in Figure 4. On the plate lower surface ($z = 10$ mm) scalar potential of electric field was taken to be constant (equal to zero); on the axis of symmetry and at sufficiently great distance from the axis ($R = 50$ mm) the radial component of current density vector was taken to be zero. Vector field of current densities $j(r, z, t_k)$ was calculated at each moment of time t_k, which was used to find $I^2(r, z, t_k)$ distribution. Average value of the respective characteristic $\langle I^2(r, z)\rangle$ was calculated by the method of numerical integration by quadrature formula of a rectangles. Effective value of vortex component of electromagnetic force was found from formula (5), and magnetic pressure created by this force — by formula (6). Results of calculation of the above characteristics are given in Figures 8, 9.

As volume density of vortex component of electromagnetic force $\vec{F}_{rot}(r, z)$ is in quadratic dependence on magnetic field intensity $H_\theta(r, z)$ (see [14]), the nature of radial distribution of $\langle \|\vec{F}_{rot}(r, z)\|\rangle$ (see Figure 8) is similar to $H_\theta(r, z)$ distribution, including the position of radius, in which maximum of vortex component of the force is reached. Maximum value of $\langle \|\vec{F}_{rot}(r, z)\|\rangle$ decreases rapidly with greater distance from the anode surface in-depth of the weld pool, becoming more than 4 times smaller at $z = 2$ mm. Magnetic pressure field turns out to be even more concentrated near the surface of metal being welded (see Figure 9). Its largest gradient is reached in a melt layer of 1 mm thickness, located directly under the pool surface.

It is of interest to compare magnetic pressure and its axial gradient in welding by modulated current with respective characteristics for constant current $I = $ const. In Figures 10, 11 the results of the respective

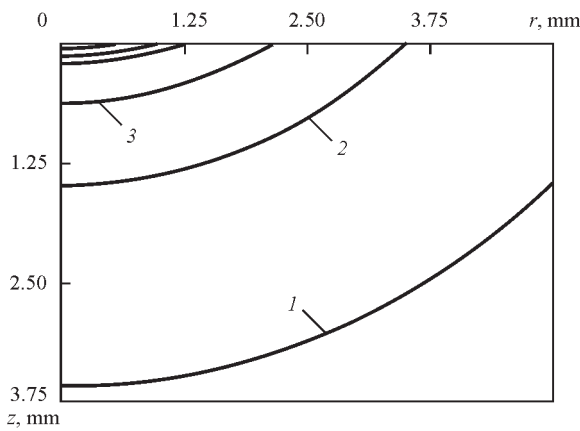**Figure 9.** Isobars of averaged magnetic pressure in the weld pool: $1 — \langle P_{mag}(r, z) \rangle = 5$; $2 — 15$; $3 — 30$ Pa (curves in the upper part of the Figure correspond to 45, 50 and 55 Pa)
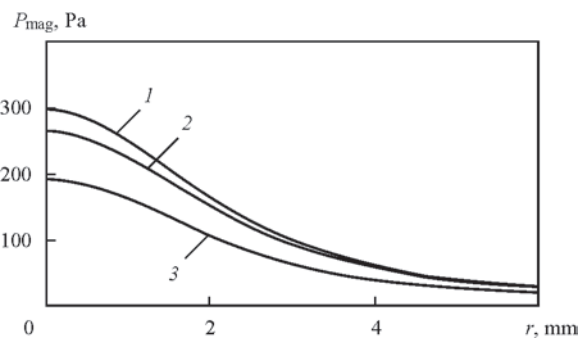

Figure 10. Distribution of magnetic pressure on weld pool surface: $\langle P_{mag} \rangle$ for an arc of modulated current (curve *1*); P_{mag} for stationary arcs at $I = I_E = 175$ A (curve *2*) and $I = I_A = 140$ A (curve *3*)

calculations at $I = I_A = 140$ A and $I = I_E = 175$ A are given in comparison with characteristics for the case of modulated current. As expected, magnetic pressure at modulated current welding is significantly higher than magnetic pressure of constant current, coinciding in value with average value of modulated current. However, $\langle P_{mag} \rangle$ exceeding P_{mag} at $I = I_E = 175$ A requires some clarification. The cause for this excess are dynamic processes in the arc, flowing in high-frequency modulated current welding, in particular extreme behaviour of current density on the pulse leading front (see Figures 5, 6).

Note that in the considered case maximum value of magnetic pressure is equal to less than 0.1 % of atmospheric pressure. However, because of its high concentration near the weld pool surface, the radial, and particularly, axial components of magnetic pressure gradient turn out to be quite significant (see Figures 9, 11).

Let us illustrate the last statement. For this purpose we will use the equation of movement of viscous incompressible fluid in the cylindrical system of coordinates (r, z), which is the projection of the balance of volume forces on axis z. We will assume melt movement to be stationary, and pressure in the liquid phase to be averaged magnetic pressure $\langle P_{mag} \rangle$. Let us denote vector of liquid metal movement speed as $\vec{V}(r, z)$; and ρ as its density. As a result, we obtain:

$$\rho \left(V_r \frac{\partial V_z}{\partial r} + V_z \frac{\partial V_z}{\partial z} \right) = -\frac{\partial \langle P_{mag} \rangle}{\partial z} + \nu \Delta V_z. \qquad (7)$$

We will take into account that at $r = 0$, in view of the conditions of axial symmetry of the considered flow, radial component of speed vector is equal to zero; then, neglecting the forces of viscous friction, from (7) we obtain

$$\frac{\rho}{2} \frac{\partial \overline{V}_z^2}{\partial z} = -\frac{\partial \langle \tilde{P}_{mag} \rangle}{\partial z},$$

which yields Bernoulli equation for an ideal liquid:

$$\frac{\rho}{2} \left[V_z^2(0, z) - V_z^2(0, 0) \right] = \langle P_{mag}(0, 0) \rangle - \langle P_{mag}(0, z) \rangle.$$

As axial component of speed of metal movement on pool surface ($z = 0$) can be considered equal to zero, Bernoulli equation yields a simple formula for approximate estimation of axial speed of melt flowing on the pool axis of symmetry ($r = 0$):

$$V_z(0, z) = \sqrt{\frac{2 \left(\langle P_{mag}(0, 0) \rangle - \langle P_{mag}(0, z) \rangle \right)}{\rho}}. \qquad (8)$$

Results of calculation by this formula for steel, given in Figure 12, are indicative of the fact that quite intensive downward (directed towards pool bottom) melt flow arises in the weld pool under the impact of magnetic pressure gradient, which is capable of transporting overheated metal from the hottest subsurface region in-depth of the melt, and thus increasing penetration depth, this effect being the most pronounced at pulse modulation of welding current.

Discussion of results. Effective value of modulated current does not directly determine the number of charges, transferred per a unit of time through the conductor cross-section, but is an indirect parameter, which characterizes thermal and force impact of current on the conducting medium in comparison with the impact of constant current of the respective magnitude.
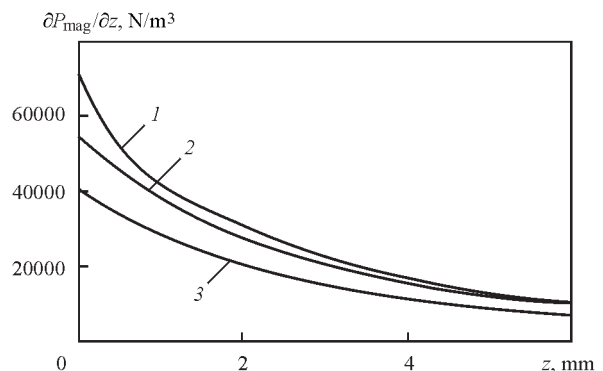

Figure 11. Distribution of axial value of axial component of magnetic pressure gradient: $1 — I = I(t)$ (modulated current): $2 — I = I_A = 140$ A; $3 — I = I_E = 175$ A
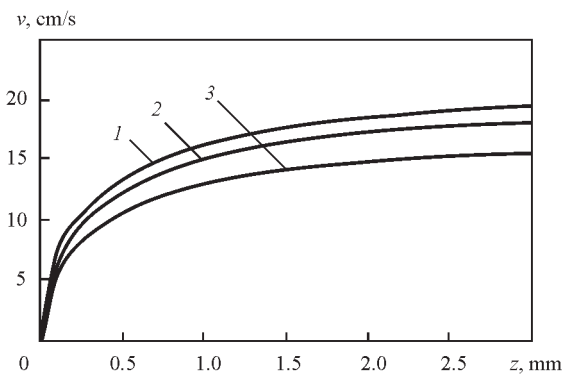
Figure 12. Axial change of axial component of the vector of weld pool metal movement speed ($\rho = 7040$ kg/m^3, designations on the curves are the same as in Figure 11)

However, these two kinds of impact are exactly the most significant ones for the technological results of arc welding, primarily, in terms of their influence on the depth and shape of metal penetration. Therefore, theoretical analysis of processes running in arc plasma, and in the metal being welded, appears to be very important for revealing the hidden capabilities of TIG welding with high-frequency pulse current modulation.

Conducted in section 1 analysis of the dependence of effective value of modulated current on modulation mode parameters is indicative of the fact that this characteristic is independent of modulation frequency, and is determined only by the shape and relative duration of current pulses. This almost obvious result is also valid for other pulse shapes, different from the trapezoidal one considered here. At selected value of average current, the highest effective value of current can be ensured through appropriate selection of time parameters of pulse modulation, and, therefore, greater force and thermal impact of modulated current both on arc plasma, and on weld pool metal. It should be noted that effective value of modulated current, as its integral characteristic, does not uniquely define thermal power of the arc discharge, as arc voltage also depends on current, changing during current pulse passage. In [19] it is shown that dynamic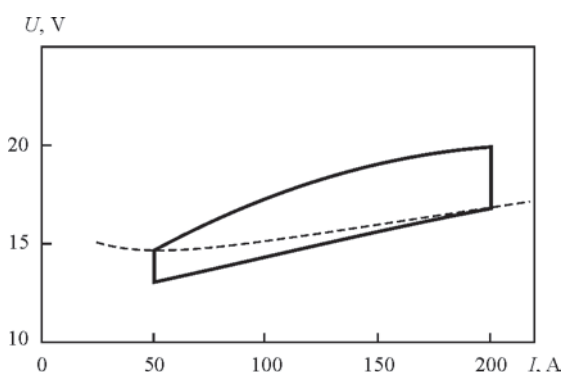 volt-ampere characteristic of nonstationary arc forms a hysteresis loop (see also [13]), enclosing (Figure 13) the volt-ampere characteristic of constant current arc. The shorter the duration of pulse leading front, the greater the loop of hysteresis loop, and, therefore, the greater the difference between the power of nonstationary arc and that of constant current arc, coinciding in magnitude with effective value of modulated current. Therefore, in high-frequency arc welding effective value of arc power should be determined by averaging the product of instantaneous values of current and voltage. At digital measurement of current and voltage with computer recording of signals, determination of average electric power of modulated current is not difficult. Theoretical analysis of this characteristic, however, requires use of arc discharge model with description of both arc column, and its near-electrode regions. Investigations in this direction are still to be performed, including experimental ones.

The conclusion that effective current value is independent of modulation frequency does not at all mean that value F has no influence on thermal and hydrodynamic processes, running in the metal being welded. In the second section it is established that force interaction of modulated current with intrinsic magnetic field is determined not by square of effective current value, but by its analog distributed in the metal volume, which is value $\langle I^2(r, z)\rangle$ — square of effective value of current flowing in a circle of radius r. This characteristic is highly dependent on modulation frequency F, as at high-frequency modulation of current by pulses with a steep leading front $\langle I^2(r, z)\rangle$ distribution is influenced by the above-described dynamic processes in the arc column and anode region, manifested in extreme distribution of current density at the anode (see Figures 5, 6). This, eventually, determines the difference between the force impact on the metal being welded of the arc with pulse current modulation and arc at constant current, coinciding by magnitude with effective value of modulated current (see Figures 11, 12).

It should be noted that given in this work results of calculations of the characteristics of electromagnetic processes in the metal being welded, were obtained in the assumption that the sample being welded is firmly pressed against the copper backing (electric potential of the sample lower surface is taken to be constant). Other variants of sample grounding were also considered during performance of computational experiments. Here, the pattern of current distribution in the metal being welded was cardinally different, depending on the position of local grounding relative to arc axis. Despite that, quantitative characteristics of force impact of modulated current on the metal being welded, given in the second section, remain valid for different connection diagrams. This result is due to

Figure 13. Dynamic volt-ampere characteristic of stationary argon arc 3 mm long with 20 μs duration of the pulse leading front

high concentration of the field of magnetic pressure in the subsurface layer of weld pool metal approximately 1 mm thick (see Figure 9). In this layer distribution of current density and configuration of current lines are determined only by distribution of electric current density on the pool surface and are weakly dependent on the pattern of current spreading in the entire sample being welded.

In work [14] it is shown that technological means, providing a reduction of the size of the arc anode binding region (increase of electric current density on weld pool surface) in TIG welding, promote an increase of axial component of magnetic pressure in paraxial regions of the pool, and lead to intensification of downward flow of the melt, respectively, thus facilitating increase of penetration depth of the metal being welded. Analysis of effective values of electromagnetic characteristics of nonstationary arc in TIG welding performed in this study, gives grounds to assert that application of high-frequency pulse modulation of welding current is one of such technological means.

Finally, we will note one more important feature of the impact of vortex component of the Lorentz force on formation of magnetic pressure field in the weld pool. The action of centripetal force $\vec{F}_{rot}(r, z)$, as well as the distribution of magnetic field intensity $H_\theta(r, z)$, extends to unlimited space. Having reached the maximum value (see Figure 8), both these characteristics of electromagnetic field tend to zero as $1/r$. On the other hand, magnetic pressure in the weld pool forms under the impact of just that part of force $\vec{F}_{rot}(r, z)$, , which is applied to molten metal; now the rest of the force is balanced by elastic reaction of the solid phase. Therefore, the smaller the pool cross-section, the smaller the fraction of welding current flowing through it, and the lower its force impact, respectively. This, on the whole, correct conclusion, is not obvious in the case, when reduction of pool cross-section is due to electric current contraction on anode surface under the impact of additional technological factors, such as application of activating fluxes, special shielding gas mixtures, or focused laser radiation (hybrid TIG + CO_2-laser welding), as at constriction of the current channel on anode surface the fraction of current flowing through the weld pool becomes greater. Clarifying the physical features of force impact of arc current under the conditions of this alternative is the subject of further research. It is also of interest to study the possibility of increasing the force impact of arc current on weld pool metal due to dynamic effects, arising in electric current density distribution on anode surface at passing of very steep leading front of the pulse. Therefore, another object of further studies

are dynamic processes in the arc discharge and metal being welded at current modulation by rectangular pulses, which, as is shown in the first section, have an advantage over triangular pulses in terms of effective current value.

1. Leitner, R.E., McElhinney, G.H., Pruitt, E.L. (1973) An investigation of pulsed GTA welding variables. *Welding J., Res. Suppl.*, **9**, 405–410.
2. Omar, A.A., Lundin, C.D. (1979) Pulsed plasma-pulsed GTA arcs: A study of the process variables. *Ibid.*, **4**, 97–105.
3. Cook, G.T., H.E.E.H. EASSA (1985) The effect of high-frequency pulsing of a welding arc. *IEEE Transact. Ind. Appl.*, 1A-21, **5**, 1294–1299.
4. Kolasa, A., Matsunawa, A., Arata, Y. (1986) Dynamic characteristics of variable frequency pulsed TIG arc. *Transact. of JWRI*, 15(**2**), 173–177.
5. Saedi, H.R., Unkel, W. (1988) Arc and weld pool behavior for pulsed current GTAW. *Welding J., Res. Suppl.*, **11**, 247–255.
6. Kim, W.H., Na, S.J. (1998) Heat and fluid flow in pulsed current GTA weld pool. *Int. J. Heat and Mass Transfer*, 41(**21**), 3213–3227.
7. Wu, C.S., Zheng, W., Wu, L. (1999) Modelling the transient behaviour of pulsed current tungsten-inert-gas weld pools. *Modelling Simul. Mater. Sci. Eng.*, 7(**1**), 15–23.
8. Onuki, J., Anazawa, Y., Nihei, M. et al. (2002) Development of a new high-frequency, high-peak current power source for high constricted arc formation. *Jpn. J. Appl. Phys.*, **41**, 5821–5826.
9. Traidia, A., Roger, F., Guyot, E. (2010) Optimal parameters for pulsed gas tungsten arc welding in partially and fully penetrated weld pools. *Int. J. Therm. Sci.*, **49**, 1197–1208.
10. Traidia, A., Roger, F. (2011) Numerical and experimental study of arc and weld pool behaviour for pulsed current GTA welding. *Int. J. Heat and Mass Transfer*, **54**, 2163–2179.
11. Qi, B.J., Yang, M.X., Cong, B.Q. et al. (2013) The effect of arc behavior on weld geometry by high-frequency pulse GTAW process with 0Cr18Ni9Ti stainless steel. *Int. J. Adv. Manuf. Technol.*, **66**, 1545–1553.
12. Yang, M., Yang, Z., Cong, B. et al. (2014) A study on the surface depression of the molten pool with pulsed welding. *Welding J., Res. Suppl.*, 93(**8**), 312–319.
13. Sydorets, V.N., Krivtsun, I.V., Demchenko, V.F. et al. (2016) Calculation and experimental research of static and dynamic volt-ampere characteristics of argon arc with refractory cathode. *The Paton Welding J.*, **2**, 2–8.
14. Demchenko, V.F., Krivtsun, I.V., Krikent, I.V. et al. (2017) Force interaction of arc current with self-magnetic field. *Ibid.*, **3**, 15–24.
15. Landau, L.D., Lifshits, E.M. (1982) Electrodynamics of continuums. Vol. 8. *Teoreticheskaya Fizika*, Moscow: Nauka.
16. Krivtsun, I.V., Demchenko, V.F., Krikent, I.V. (2010) Model of the processes of heat, mass and charge transfer in the anode region and column of the welding arc with refractory cathode. *The Paton Welding J.*, **6**, 2–9.
17. Krivtsun, I.V., Krikent, I.V., Demchenko, V.F. (2013) Modelling of dynamic characteristics of a pulsed arc with refractory cathode. *Ibid.*, **7**, 13–23.
18. Krivtsun, I.V., Krikent, I.V., Demchenko, V.F. (2015) Interaction of CO_2-laser radiation beam with electric arc plasma in hybrid (laser + TIG) welding. *Ibid.*, **3/4**, 6–15.
19. Sokolov, O.I., Gladkov, E.A. (1977) Dynamic characteristics of free and constricted alternating current welding arcs with non-consumable electrode. *Svarochn. Proizvodstvo*, **4**, 3–5.